LETTER

doi:10.1038/nature09999

A novel tumour-suppressor function for the Notch pathway in myeloid leukaemia

Apostolos Klinakis[1]*, Camille Lobry[2]*, Omar Abdel-Wahab[3], Philmo Oh[2], Hiroshi Haeno[4], Silvia Buonamici[2,8], Inge van De Walle[5], Severine Cathelin[2], Thomas Trimarchi[2], Elisa Araldi[2], Cynthia Liu[2], Sherif Ibrahim[2], Miroslav Beran[6], Jiri Zavadil[7], Argiris Efstratiadis[1], Tom Taghon[5], Franziska Michor[4], Ross L. Levine[3] & Iannis Aifantis[2]

Notch signalling is a central regulator of differentiation in a variety of organisms and tissue types[1]. Its activity is controlled by the multi-subunit γ-secretase (γSE) complex[2]. Although Notch signalling can play both oncogenic and tumour-suppressor roles in solid tumours, in the haematopoietic system it is exclusively oncogenic, notably in T-cell acute lymphoblastic leukaemia, a disease characterized by Notch1-activating mutations[3]. Here we identify novel somatic-inactivating Notch pathway mutations in a fraction of patients with chronic myelomonocytic leukaemia (CMML). Inactivation of Notch signalling in mouse haematopoietic stem cells (HSCs) results in an aberrant accumulation of granulocyte/monocyte progenitors (GMPs), extramedullary haematopoieisis and the induction of CMML-like disease. Transcriptome analysis revealed that Notch signalling regulates an extensive myelomonocytic-specific gene signature, through the direct suppression of gene transcription by the Notch target *Hes1*. Our studies identify a novel role for Notch signalling during early haematopoietic stem cell differentiation and suggest that the Notch pathway can play both tumour-promoting and -suppressive roles within the same tissue.

Notch is essential for the emergence of definitive haematopoiesis[4], controls HSC differentiation to the T-cell lineage[5,6] and is a major oncogene, as most patients with T-cell acute lymphoblastic leukaemia harbour activating *Notch1* mutations[7]. To study haematopoiesis in the absence of any Notch-derived signal (as mammals express four different Notch receptors), we targeted Nicastrin (*Ncstn*), a member of the γSE complex and one of the few non-redundant members of the pathway (Supplementary Fig. 1). We crossed the $Ncstn^{f/f}$ mice to both an inducible (Mx1-cre)[8] and a haematopoietic-specific (Vav-cre)[9] recombinase strain. Both modes of deletion (referred to herein as $Ncstn^{-/-}$) produced identical phenotypes. Unexpectedly, none of the $Ncstn^{-/-}$ mice survived longer than 20 weeks. Further analysis revealed a striking peripheral blood leukocytosis and monocytosis with enlargement of the spleen (Fig. 1a, b and Supplementary Figs 2 and 3). Histological analysis of the spleen showed a marked expansion of the red pulp with diffuse infiltration by myeloid and monocytic cells. The infiltrating myeloid cells were partly myeloperoxidase positive and $CD11b^+$ and/or $Gr1^+$ (Fig. 1b and Supplementary Figs 2 and 3). The increase in monocyte numbers was also observed in the bone marrow and liver (Fig. 1a and data not shown). Taken together, these findings were diagnostic for a myeloproliferative/myelodysplastic process and reminiscent of human CMML. CMML is a myeloid malignancy, classified as a myeloproliferative disorder/myelodysplastic syndrome overlap, which is characterized by monocytosis, myeloproliferation, variable bone marrow dysplasia and a high rate of progression to acute myeloid leukaemia[10].

Because monocytes and granulocytes originate from the GMP subset, we examined the stem and progenitor cell populations in the bone marrow. *Ncstn* deletion lead to an enlargement of the $Lineage^{neg}Sca1^+c\text{-}Kit^+$ (LSK), specifically the LSK $CD150^+CD48^+$ subset, a population shown to have a myeloid commitment bias[11]. This differentiation bias was coupled to a significant reduction of the lymphoid-biased multipotential progenitor population (L-MPP)[12] (Supplementary Fig. 4). Moreover, there was a striking increase in the absolute numbers of both bone marrow and spleen GMP cells (Fig. 1d) coupled to a decrease of the megakaryocyte–erythrocyte progenitor population. This apparent predisposition towards GMP-derived lineages was also evident *in vitro*, as $Ncstn^{-/-}$ progenitors generated more granulocyte–macrophage and macrophage colonies (Supplementary Fig. 5). Further studies also revealed a striking ability of the $Ncstn^{-/-}$ progenitors to replate serially (Supplementary Fig. 6), suggesting an increase in their self-renewal potential. Consistent with this idea, whole transcriptome profiling of $Ncstn^{-/-}$ GMP progenitors revealed enrichment of a 'leukemic self-renewal' signature[13]. Finally, bone marrow transplantation assays demonstrated that the effects of *Ncstn* deletion were cell autonomous (Supplementary Fig. 7)[14].

Although the γSE complex has other substrates[2], we focused on Notch signalling because of our finding that *Ncstn* deletion led to known $Notch^{-/-}$ phenotypes, including a block in T-cell differentiation (Supplementary Fig. 8)[15]. To prove a connection to Notch signalling, we generated animals that conditionally lack the expression of three out of four Notch receptors ($Mx1\text{-}cre^+N1^{f/f}N2^{f/f}N3^{-/-}$)[16]. Strikingly, triple *Notch1/2/3* deletion copied the $Ncstn^{-/-}$ phenotypes (Supplementary Fig. 9). $Notch1\text{–}3^{-/-}$ mice developed both CMML-like symptoms, and significant enlargement of the GMP population. *Notch3* expression was dispensable, as simultaneous deletion of only *Notch1* and *Notch2* led to an identical CMML-like pathology. However, introduction of a single wild-type (WT) *Notch1* or *Notch2* allele was able to suppress the disease phenotype. Consistent with the importance of Notch1–2 receptor signalling in these stages, quantitative PCR studies revealed expression of *Notch1* and *Notch2*, but not *Notch3*, in WT stem and progenitor cells (Supplementary Fig. 10).

We next sought to delineate the mechanism by which Notch directs the regulation of early haematopoiesis. Deletion of *Ncstn* did not lead to any alterations in the GMP cell-cycle status or cell death rate (not shown). We hypothesized that γSE complex/Notch signals actively suppress a GMP-specific gene expression program. We sorted LSK and GMP cells and studied their transcriptome. This analysis revealed a statistically significant de-repression of an extended myeloid-specific program[12] in $Ncstn^{-/-}$ LSK cells (Fig. 2a and Supplementary Fig. 11).

[1]Biomedical Research Foundation, Academy of Athens, Athens, Greece. [2]Howard Hughes Medical Institute and Department of Pathology, New York University School of Medicine, New York, New York 10016, USA. [3]Human Oncology and Pathogenesis Program and Leukemia Service, Department of Medicine, Memorial Sloan-Kettering Cancer Center, New York, New York 10016, USA. [4]Department of Biostatistics and Computational Biology, Dana-Farber Cancer Institute, and Department of Biostatistics, Harvard School of Public Health, Boston, Massachusetts 02115, USA. [5]Department of Clinical Chemistry, Microbiology and Immunology, Ghent University Hospital, Ghent University, Ghent, Belgium. [6]Department of Leukemia, M.D. Anderson Cancer Center, Houston, Texas 77030, USA. [7]Department of Pathology, NYU Cancer Institute and Center for Health Informatics and Bioinformatics, NYU Langone Medical Center, New York, New York 10016, USA. [8]Novartis Institutes for Biomedical Research, Cambridge, Massachusetts 02139, USA.
*These authors contributed equally to this work.

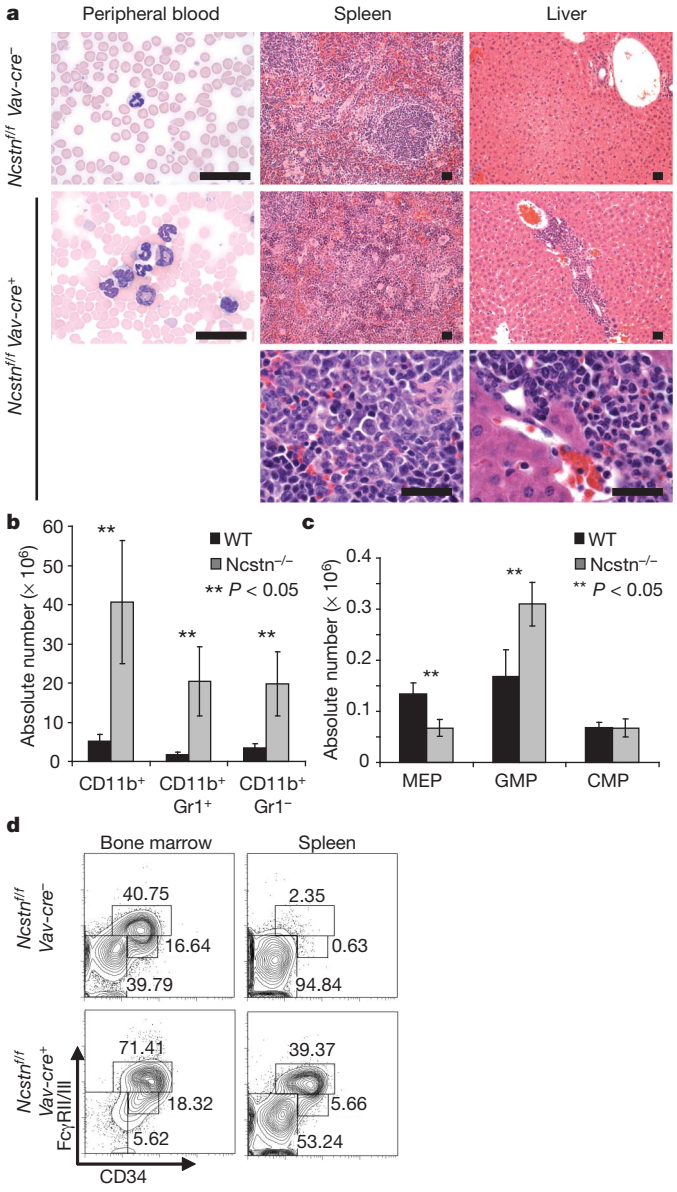

Figure 1 | *Ncstn* deficiency leads to CMML-like disease and a significant enlargement of the GMP progenitor population. **a**, Histological analysis showing accumulation of monocytes and granulocytes in peripheral blood (Wright–Giemsa staining), spleen and liver (haematoxylin and eosin staining). A magnification of each infiltrant is shown in the lowest panels. **b**, Absolute numbers of each monocytic/granulocytic subset from the spleen of control and *Ncstn*$^{f/f}$ *Vav-cre*$^{+}$ littermate animals (12 weeks of age, mean ± s.d., $n = 10$). **c**, Absolute numbers of each progenitor subpopulation in the bone marrow (mean ± s.d., $n = 10$). **d**, Detailed FACS analysis of bone marrow and spleen myeloid progenitor (myeloid progenitors: Lin^{-}/c-Kit^{+}/Sca-1^{-}) populations of *Ncstn*$^{f/f}$ *Vav-cre*$^{+}$ and *Ncstn*$^{f/f}$ *Vav-cre*$^{-}$ littermates showing a significant enlargement of the GMP (FcγRII/III^{+}, CD34^{+}) subset.

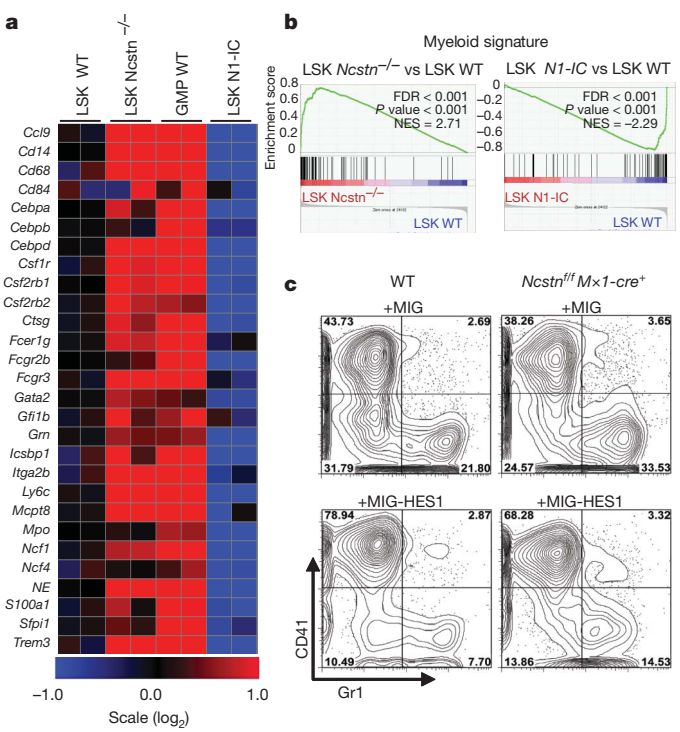

Figure 2 | Notch signalling suppresses an extensive myeloid gene expression program through the induction of the transcriptional repressor Hes1. **a**, Heat map showing regulation of genes representative of the myeloid signature from the indicated cell populations and mice. **b**, Expression data were analysed for lists of genes positively involved in myelopoiesis using gene-set enrichment analysis. Enrichment plots show upregulation of myeloid-specific genes in *Ncstn*$^{f/f}$*Mx1-cre*$^{+}$ and downregulation in Notch1^{IC} *Mx1-cre*$^{+}$ LSK cells (compared with WT counterparts). **c**, Purified cKit^{+} progenitors from WT and *Ncstn*$^{f/f}$*Mx1-cre*$^{+}$ mice were transduced with retroviruses encoding Hes-1 or empty vector, subsequently plated on methylcellulose for 7 days and analysed for expression of myeloid or megakaryocyte differentiation markers (Gr1, CD41). A representative of four experiments is shown.

Gene-set enrichment analysis demonstrated a significant enrichment of myeloid-specific gene-sets within the *Ncstn*$^{-/-}$ LSK gene signature (Fig. 2b and Supplementary Table 1). Further dissection of the LSK subset showed that the GMP gene expression program was initiated as early as the CD150^{+} HSC stage of differentiation, and persisted at the CD150^{-} subset, which included MPPs (Supplementary Fig. 11). Furthermore, we were able to show that gene expression in LSKs purified from an inducible Notch1 gain-of-function genetic model (*Ef1α1-lsl-Notch1*^{IC}*Mx1-cre*$^{+}$)[17] was inversely correlated with the loss-of-function signature seen in *Ncstn*$^{-/-}$ LSK progenitors (Fig. 2a). Notch1^{IC} expression led to suppression of myeloid-specific genes, suggesting that activation of Notch signalling can alter the transcription and differentiation of uncommitted HSC and MPP cells. Gene-set enrichment analysis further supported these findings as it showed a negative correlation between the Notch1^{IC} LSKs and previously reported myeloid gene expression signatures (Fig. 2a, b, Supplementary Table 2 and Supplementary Fig. 11).

As Notch is thought to function primarily as a transcriptional activator, we hypothesized that its suppressive effects on GMP-specific gene expression could be explained by the induction of a transcriptional repressor. A search for such a molecule revealed *Hes1*, a known Notch target and a transcriptional repressor (Supplementary Fig. 11a). Interestingly, *Hes1* was previously suggested to play a role in myeloid leukaemia, as a downstream effector of the *Junb* tumour suppressor in an animal model of chronic myeloid leukemia[18]. To test the potential involvement of *Hes1* directly, we used *in vitro* differentiation assays and showed that *Hes1* ectopic expression was sufficient to direct differentiation away from the granulocyte/monocyte lineage (Fig. 2c). Furthermore, *Hes1* expression suppressed the expression of key granulocyte/monocyte commitment genes such as *Cebpa* and *Pu.1* (Supplementary Fig. 12a). In agreement with this finding, we identified putative *Hes* (N-box) binding sites on the promoters of both genes. Reporter and chromatin immunoprecipitation assays proved direct binding of Hes1 on these promoters and suppression of transcription (Supplementary Fig. 12b–e).

These findings suggested that Notch (or Hes1) hyper-activation could suppress CMML-like disease developing in *Ncstn*$^{-/-}$ animals. To test this, we used the previously described *Ef1α1-lsl-Notch1*$^{IC+}$ mice[17]. We generated *Notch1*^{IC}*Ncstn*$^{f/f-}$*Mx1-Cre*$^{+}$ animals and analysed both GMP accumulation and disease progression. Notch1^{IC} expression was

sufficient to suppress both GMP expansion and disease development significantly (Fig. 3a, b and Supplementary Fig. 13). Interestingly, Notch1^{IC} expression drove progenitor commitment towards the lymphoid (T cell) and megakaryocyte–erythrocyte progenitor lineages[19]. However, Notch1^{IC} expression did not affect cell-cycle kinetics within the GMP subset (Supplementary Fig. 13). To uncouple differentiation to the GMP subset from effects on GMP homeostasis, we purified WT GMP and plated them on stroma in the presence or absence of Notch ligands (Dll1 and Dll4). A striking increase of apoptosis rate was noted in the presence of Dll1–4 (Fig. 3c). These experiments suggest that Notch ectopic expression can affect both the commitment to the GMP subset and the survival of already committed GMP progenitors.

Our studies so far demonstrate that Notch controls murine myelopoiesis and that its deletion leads to GMP expansion and monocytic disease. To prove that Notch is also important in human haematopoiesis and leukemogenesis, we initially cultured purified human CD34$^+$CD38$^-$Lin$^-$ bone marrow and cord blood stem and progenitor cells on stroma expressing different Jagged and Delta-like Notch ligands[20]. We found that expression of Notch ligands efficiently suppressed differentiation of human multipotential progenitors towards both the granulocyte (CD15$^+$) and monocyte (CD14$^+$) lineages (Supplementary Figs 14 and 15). This suppression was prevented when the activity of the γSE complex was suppressed using either small molecule inhibitors or by the expression of a dominant negative *MAML1* mutant.

To gain further insights into the role of Notch in human CMML, we extensively sequenced many γSE/Notch pathway genes. Exon resequencing of specimens from patients with CMML (Supplementary Table 3) identified a substantial fraction (six novel mutations in 5 out of 42 patients) harbouring somatic heterozygous mutations in multiple Notch pathway genes including *NCSTN*, *APH1*, *MAML1* and *NOTCH2* (Fig. 4 and Supplementary Table 4). In addition, several other putative mutations (single nucleotide variants) were detected, which are not annotated as known germline single nucleotide polymorphisms but for which we could not prove a somatic origin (Supplementary Table 5). The validated somatic mutations were only observed in CMML, as re-sequencing of 47 samples from patients with myeloproliferative disorders (polycythemia vera or myelofibrosis) did not reveal somatic mutations in the Notch pathway (Fig. 4b). Importantly, CMML specimens with Notch mutations also had somatic alterations in well-characterized myeloid oncogenic lesions[21],

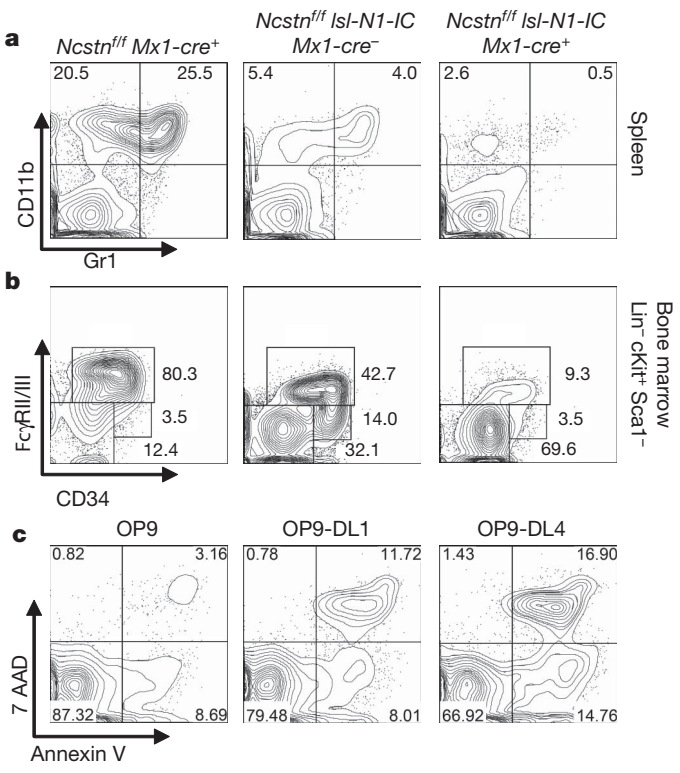

Figure 3 | Ectopic expression of Notch1-IC is able to prevent CMML-like disease in *Ncstn*$^{-/-}$ mice. **a**, PolyI:polyC-induced Notch1-IC expression in *Ncstn*$^{f/f}$*lsl-N1-IC Mx1-Cre*$^+$ animals suppresses myeloid cells in spleen. **b**, Notch1-IC expression suppresses GMP progenitor population in bone marrow. **c**, Induction of cell death in WT GMP cells cultured in the presence (OP9-DL1-4) or absence (OP9) of Notch ligands. Cell death was measured by the combination of 7AAD and annexin V staining 48 h after co-culture initiation. For **a**–**c**, a representative of more than three experiments is shown.

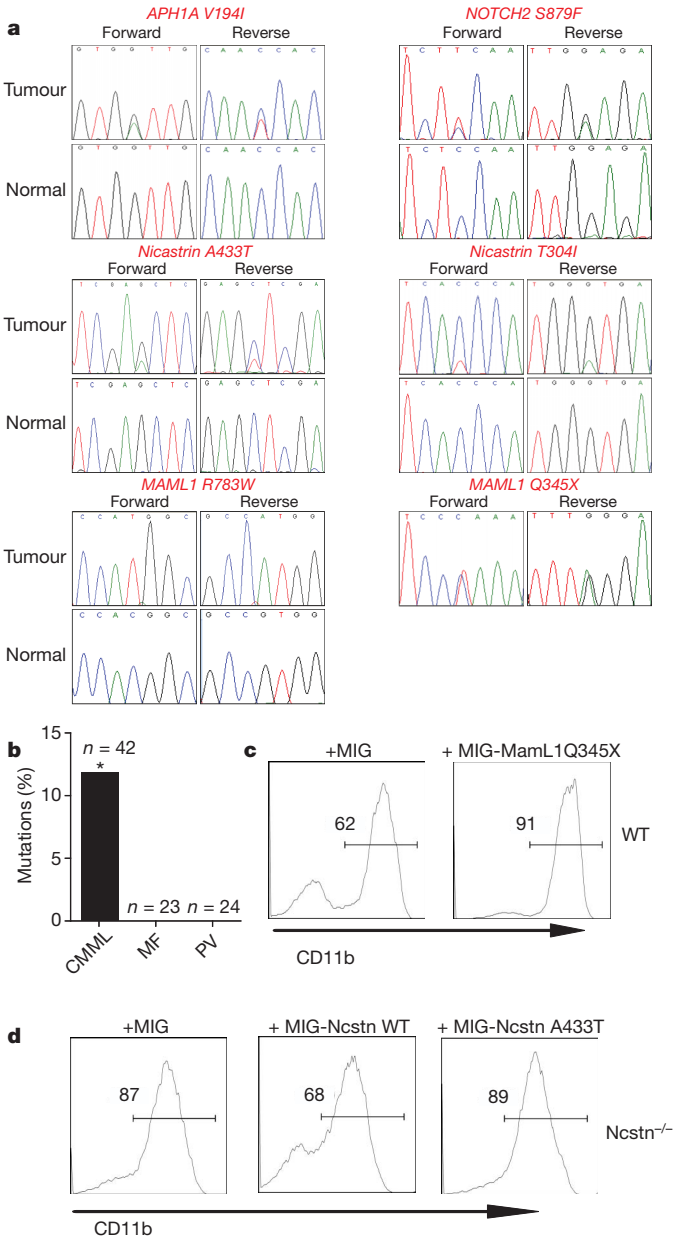

Figure 4 | Novel, loss-of-function Notch pathway mutations in human CMML. **a**, Sequence traces of identified Notch pathway mutations in tumours from patients with CMML but not in normal tissues show somatic origin. **b**, Comparison of the percentage of Notch pathway mutations in specimens from patients with CMML, myelofibrosis and polycythemia vera. The asterisk denotes that only verified somatic CMML mutations are included. **c**, OP9-DL1 co-culture of WT LSK cells infected with specified constructs. Analysis of the CD11b$^+$ population was studied 14 days after the initiation of the culture. **d**, A similar experiment as in **c**, using LSK *Ncstn*$^{-/-}$ progenitors infected with the specified constructs. In all cases, a representative of more than three experiments is shown.

including *JAK2*, *KRAS*, *TET2* and *ASXL1*, suggesting mutational cooperation between Notch signalling and other oncogenic pathways in CMML (Supplementary Table 4). We then asked if those mutations were causally related with the disease by using transcriptional reporter and *in vitro* differentiation assays. We demonstrated that selected mutations had the ability to affect Notch activity negatively either as dominant negative (MAML1Q345X) or null (NCSTNA433T) alleles (Fig. 4c, d and Supplementary Fig. 16). This is the first description, to our knowledge, of somatic Notch pathway loss-of-function mutations in human cancer.

The presented studies identify novel inactivating Notch pathway mutations and suggest that γSE complex/Notch signalling controls early HSC/MPP commitment decisions in bone marrow. A significant portion of this regulation is controlled by the Hes family of transcriptional repressors. Most importantly, our studies suggest that silencing Notch activity leads to the development of myeloid leukaemia, implying a novel tumour-suppressor function for the Notch pathway in haematopoiesis. Although mutation-mediated pathway silencing can be found in CMML, it is conceivable that there are additional control mechanisms, including epigenetic silencing of Notch pathway target genes. Whatever the mode of regulation, our observations suggest that reversible activation of the Notch pathway may represent an attractive future therapy, targeting specifically the progression and relapse of granulocytic and monocytic neoplasms.

METHODS SUMMARY

Animals. All mice were kept in specific pathogen-free animal facilities at the New York University School of Medicine. Mx1-Cre^{+} animals were injected with 20 μg polyI:polyC per gram of body weight for a total of six injections. The injections were initiated 14 days after birth and done every 2 days. Animals were analysed 4–6 weeks after the last injection unless indicated otherwise. All animal experiments were done in accordance to the guidelines of the New York University School of Medicine Institutional Animal Care and Use Committee.

Antibodies and fluorescence-activated cell sorting analysis. Antibody staining and fluorescence-activated cell sorting (FACS) were performed as previously described[22]. All antibodies were purchased from BD-Pharmingen or e-Bioscience. We used the following antibodies: c-kit (2B8), Sca-1 (D7), Mac-1 (M1/70), Gr-1 (RB6-8C5), NK1.1 (PK136), TER-119, CD3 (145-2C11), CD19 (1D3), IL7Rα (A7R34), CD34 (RAM34), FcγRII/III (2.4G2), Flk-2/Flt-3 (A2F10.1), CD4 (RM4-5), CD4 (H129.19), CD8 (53-6.7), CD45.1 (A20), CD45.2 (104), CD150 (9D1), CD48 (HM481). Bone marrow lineage antibody cocktail included Mac-1, Gr-1, NK1.1, TER-119, CD3 and CD19.

OP9-DL1/DL4 *in vitro* co-culture. OP9-DL1/DL4 cells were maintained in MEM with 20% fetal bovine serum. Ten thousand purified infected (green fluorescent protein (GFP^{+})) LSK or cKit^{+} bone marrow progenitors were seeded into a six-well plate with confluent OP9 cells in the presence of 10 ng ml^{-1} SCF, 10 ng ml^{-1} interleukin-3 (IL-3), 5 ng ml^{-1} Flt3-L, 10 ng ml^{-1} IL6 and 5 ng ml^{-1} IL-7. Flow cytometric analysis was performed on an LSRII (BDIS). Haematopoietic cells were gated using CD45 cell-surface expression.

Microarray analysis. LSK or GMP cells from individual mice were used. To generate sufficient sample quantities for oligonucleotide gene chip hybridization, we used the Ovation RNA Amplification System V2 (Nugen) for antisense RNA (cRNA) amplification and labelling. The amplified cRNA was labelled and hybridized to the Mouse 430.2 microarrays (Affymetrix). The data were normalized using the previously published robust multi-array average algorithm using the GeneSpring GX software (Agilent).

Full Methods and any associated references are available in the online version of the paper at www.nature.com/nature.

Received 8 August 2010; accepted 14 March 2011.

1. Hurlbut, G. D., Kankel, M. W., Lake, R. J. & Artavanis-Tsakonas, S. Crossing paths with Notch in the hyper-network. *Curr. Opin. Cell Biol.* **19,** 166–175 (2007).
2. De Strooper, B. Nicastrin: gatekeeper of the γ-secretase complex. *Cell* **122,** 318–320 (2005).
3. Aifantis, I., Raetz, E. & Buonamici, S. Molecular pathogenesis of T-cell leukaemia and lymphoma. *Nature Rev. Immunol.* **8,** 380–390 (2008).
4. Robert-Moreno, A. *et al.* Impaired embryonic haematopoiesis yet normal arterial development in the absence of the Notch ligand Jagged1. *EMBO J* **27,** 1886–1895 (2008).
5. Zuniga-Pflucker, J. C. T-cell development made simple. *Nature Rev. Immunol.* **4,** 67–72 (2004).
6. Rothenberg, E. V. & Taghon, T. Molecular genetics of T cell development. *Annu. Rev. Immunol.* **23,** 601–649 (2005).
7. Grabher, C., von Boehmer, H. & Look, A. T. Notch 1 activation in the molecular pathogenesis of T-cell acute lymphoblastic leukaemia. *Nature Rev. Cancer* **6,** 1–13 (2006).
8. Kuhn, R., Schwenk, F., Aguet, M. & Rajewsky, K. Inducible gene targeting in mice. *Science* **269,** 1427–1429 (1995).
9. Stadtfeld, M. & Graf, T. Assessing the role of hematopoietic plasticity for endothelial and hepatocyte development by non-invasive lineage tracing. *Development* **132,** 203–213 (2005).
10. Emanuel, P. D. Juvenile myelomonocytic leukemia and chronic myelomonocytic leukemia. *Leukemia* **22,** 1335–1342 (2008).
11. Challen, G. A., Boles, N. C., Chambers, S. M. & Goodell, M. A. Distinct hematopoietic stem cell subtypes are differentially regulated by TGF-β1. *Cell Stem Cell* **6,** 265–278 (2010).
12. Ng, S. Y., Yoshida, T., Zhang, J. & Georgopoulos, K. Genome-wide lineage-specific transcriptional networks underscore Ikaros-dependent lymphoid priming in hematopoietic stem cells. *Immunity* **30,** 493–507 (2009).
13. Krivtsov, A. V. *et al.* Transformation from committed progenitor to leukaemia stem cell initiated by MLL-AF9. *Nature* **442,** 818–822 (2006).
14. Dumortier, A. *et al.* Atopic dermatitis-like disease and associated lethal myeloproliferative disorder arise from loss of notch signaling in the murine skin. *PLoS ONE* **5,** e9258 (2010).
15. Radtke, F. *et al.* Deficient T cell fate specification in mice with an induced inactivation of Notch1. *Immunity* **10,** 547–558 (1999).
16. Demehri, S. *et al.* Notch-deficient skin induces a lethal systemic B-lymphoproliferative disorder by secreting TSLP, a sentinel for epidermal integrity. *PLoS Biol* **6,** e123 (2008).
17. Buonamici, S. *et al.* CCR7 signalling as an essential regulator of CNS infiltration in T-cell leukaemia. *Nature* **459,** 1000–1004 (2009).
18. Santaguida, M. *et al.* JunB protects against myeloid malignancies by limiting hematopoietic stem cell proliferation and differentiation without affecting self-renewal. *Cancer Cell* **15,** 341–352 (2009).
19. Mercher, T. *et al.* Notch signaling specifies megakaryocyte development from hematopoietic stem cells. *Cell Stem Cell* **3,** 314–326 (2008).
20. Taghon, T. N., David, E. S., Zuniga-Pflucker, J. C. & Rothenberg, E. V. Delayed, asynchronous, and reversible T-lineage specification induced by Notch/Delta signaling. *Genes Dev.* **19,** 965–978 (2005).
21. Tefferi, A. Novel mutations and their functional and clinical relevance in myeloproliferative neoplasms: JAK2, MPL, TET2, ASXL1, CBL, IDH and IKZF1. *Leukemia* **24,** 1128–1138 (2010).
22. Aifantis, I., Feinberg, J., Fehling, H. J., Di Santo, J. P. & von Boehmer, H. Early T cell receptor β gene expression is regulated by the pre-T cell receptor-CD3 complex. *J. Exp. Med.* **190,** 141–144 (1999).

Supplementary Information is linked to the online version of the paper at www.nature.com/nature.

Acknowledgements We thank G. Fishel, F. Radtke and R. Kopan for donating mouse strains; P. Lopez and the New York University Flow Facility for cell sorting; and A. Heguy and the Geoffrey Beene Translational Core laboratory for assistance with DNA resequencing. The New York University Cancer Institute Genomics Facility helped with micro-array processing. This work was supported by the National Institutes of Health (RO1CA133379, RO1CA105129, R21CA141399, RO1CA149655 to I.A.; R01CA1328234 to R.L.L. and F.M.; U54CA143798 to F.M.), the Leukemia & Lymphoma Society (to I.A.), the American Cancer Society (to I.A.), the Irma T. Hirschl Trust, the Dana Foundation, The Mallinckrodt Foundation, the Alex's Lemonade Stand Foundation (to I.A.), and the Fund for Scientific Research Flanders (Fonds Wetenschappelijk Onderzoek) and its Odysseus Research Program (to T.T.). A.E. was supported by the National Cancer Institute (1P01CA97403, Project 2) and a gift from the Berrie Foundation. A.K. was supported by an EU Marie Curie International Re-integration Grant. I.v.D.W. was supported by the Institute for the Promotion of Innovation by Science and Technology in Flanders (Agentschap voor Innovatie door Wetenschap en Technologie). S.C. was supported by the Hope Street Kids Foundations and P.O. by the New York University Medical Scientist Training Program. T.T. was supported by the Fonds Wetenschappelijk Onderzoek). O.A.W. was supported by the Clinical Scholars Program at Memorial Sloan Kettering Cancer Center and by the American Society of Hematology. R.L.L. is an Early Career Award recipient of the Howard Hughes Medical Institute and is the Geoffrey Beene Junior Chair at Memorial Sloan Kettering Cancer Center. I.A. is a Howard Hughes Medical Institute Early Career Scientist.

Author Contributions I.A., C.L. and A.K. conceived the study and designed all experiments. A.K. and A.E. helped with experimental planning and generated the Ncstn$^{f/f}$ mice. C.L. performed most of the mouse experiments and *in vitro* studies aided by P.O., S.B, S.C., T.T. and E.A. R.L.L, O.A.-W. and M.B. performed and analysed human leukaemia sample exon sequencing. H.H. and F.M. helped with disease modelling and computational analysis of disease progression. I.v.D.W. and T.T. performed the human stem cell differentiation assays. C.L. and S.I. analysed mouse disease pathology. J.Z. processed and analysed gene expression data.

Author Information The microarray data are deposited in Gene Expression Omnibus of the National Center for Biotechnical Information under accession numbers GSE27794, GSE27799 and GSE27811. Reprints and permissions information is available at www.nature.com/reprints. The authors declare no competing financial interests. Readers are welcome to comment on the online version of this article at www.nature.com/nature. Correspondence and requests for materials should be addressed to I.A. (iannis.aifantis@nyumc.org) or A.K. (aklinakis@bioacademy.gr).

METHODS

Animals. Genotyping of $N1^{f/f}N2^{f/f}N3^{-/-}$ mice[23–26] was performed as previously reported. $Ncstn^{f/f}$Mx1-Cre^{+} and $N1^{f/f}N2^{f/f}N3^{-/-}$ Mx1-Cre+ animals were injected with 20 μg polyI:polyC per gram of body weight for a total of six injections. The injections were initiated 14 days after birth and done every 2 days. Animals were analysed 4–6 weeks after the last injection unless indicated otherwise. All animal experiments were done in accordance to the guidelines of the New York University School of Medicine Institutional Animal Care and Use Committee.

Generation of the $Ncstn^{f/f}$ mice. To generate a conditional *Ncstn* allele we used standard ES cell targeting approaches. Exons 5–7 of the *Ncstn* locus were targeted for Cre-dependent recombination. Removal of these exons generates an in-frame stop codon that prematurely terminates translation. As the homology region we used a 7 kb BsrGI–EcoRI genomic fragment spanning introns 2–11. A PGK–NEO cassette and a loxP site were cloned into an EcoRV site located in intron 4, whereas the second loxP site was subcloned into a unique PmlI site of intron 7. Embryonic stem cell colonies (129/sj) were screened by Southern blot of genomic DNA digested with BamHI (Supplementary Fig. 1b). Correctly targeted embryonic stem cells were injected in C57BL6 blastocysts and chimaeras were generated. After verification of germline transmission, the PGK–NEO cassette was removed using a germline Flp mouse[27]. $Ncstn^{f/f}Flp^{+}$ mice were crossed to the Mx-cre strain. Genotyping primers and probes are available upon request.

Antibodies and FACS analysis. Antibody staining and FACS analysis was performed as previously described[22]. All antibodies were purchased from BD-Pharmingen or e-Bioscience. We used the following antibodies: c-kit (2B8), Sca-1 (D7), Mac-1 (M1/70), Gr-1 (RB6-8C5), NK1.1 (PK136), TER-119, CD3 (145-2C11), CD19 (1D3), IL-7Rα(A7R34), CD34 (RAM34), FcγRII/III (2.4G2), Flk-2/Flt-3 (A2F10.1), CD4 (RM4-5), CD4 (H129.19), CD8 (53-6.7), CD45.1 (A20), CD45.2 (104), CD150 (9D1), CD48 (HM481). Bone marrow lineage antibody cocktail included Mac-1, Gr-1, NK1.1, TER-119, CD3, CD19. For western blotting, goat polyclonal anti-Nicastrin antibody (N19, sc-14369, Santa Cruz) and mouse monoclonal anti-Actin antibody (Clone C4, MAB1501R, Millipore) were used. Annexin V/7AAD staining was done using an annexin V PE detection kit (BD Pharmingen, 559763) following the manufacturer's protocol.

PCR with reverse transcription. Total RNA was isolated using the RNeasy Plus Mini Kit (Qiagen) and cDNA was synthesized using the SuperScript First-Strand Kit (Invitrogen). Quantitative PCR was performed using SYBR green iMaster and a LightCycler 480 (Roche) with the following primer sequences (melting temperature = 60 °C for all primers): *Cebpa* forward TTACAACAGGCCAGGT TTCC, *Cebpa* reverse CTCTGGGATGGATCGATTGT; *Pu.1* forward ATGGA AGGGTTTTCCCTCACCGCC, *Pu.1* reverse GTCCACGCTCTGCAGCTCTGT GAA; *Gata2* forward AACGCCTGTGGCCTCTACTA, *Gata2* reverse TCT CTTGCATGCACTTGGAG; *Cebpd* forward ATCGCTGCAGCTTCCTATGT, *Cebpd* reverse AGTCATGCTTTCCCGTGTTC; *Hes1* forward TCCAAGCTAG AGAAGGCAGAC, *Hes1* reverse TGATCTGGGTCATGCAGTTG; *Gata1* forward ACTGTGGAGCAACGGCTACT, *Gata1* reverse TCCGCCAGAGTGTT GTAGTG; *Ncstn* forward CTGGCGCGTGCACTGTATGAG, *Ncstn* reverse GGAGACGGCGATGTAGTGTTGAAG.

Bone marrow transplantation assays. Five hundred thousand bone marrow cells ($Ly5.2^{+}$) were transplanted by retro-orbital intravenous injections into lethally irradiated (960 cGy) BL6SJL ($Ly5.1^{+}$) recipient mice. Four weeks after transplantation, mice were injected with 20 μg polyI:polyC per gram of body weight for a total of six injections. Peripheral blood of recipient mice was collected at 4, 7, 9 and 12 weeks after transplantation. Recipient mice were killed 16 weeks after transplantion for analysis.

Microarray analysis. LSK or GMP cells from individual mice were used. Microarray analysis was performed as previously described[28]. Briefly, freshly isolated cells were sorted by surface marker expression, and total RNA was extracted using the RNeasy kit (Qiagen). To generate sufficient sample quantities for oligonucleotide gene chip hybridization, we used the Ovation RNA Amplification System V2 (Nugen) for cRNA amplification and labelling. The amplified cRNA was labelled and hybridized to the Mouse 430.2 microarrays (Affymetrix). The Affymetrix gene expression profiling data were normalized using the previously published robust multi-array average algorithm using the GeneSpring GX software (Agilent). The gene-expression intensity presentations were generated with Matrix2png software (http://chibi.ubc.ca/matrix2png/bin/matrix2png.cgi) or Multi Experiment Viewer software (http://www.tm4.org/mev/).

Gene set enrichment analysis. Gene set enrichment analysis was performed using Gene Set Enrichment Analysis software[29,30] (http://www.broadinstitute.org/gsea) using gene set as permutation type, 1,000 permutations and $\log_2$ ratio of classes as metric for ranking genes.

The 'myeloid signature' gene set was generated using a systematic approach based on the comparison of gene expression arrays from WT LSK and WT GMP. Genes that were significantly upregulated in GMP compared with LSK (over 1.5-fold induction $P < 0.05$) were used to define myeloid signature genes. The list was trimmed of genes of unknown function and those related to metabolism.

Other myeloid-specific gene sets used in the analysis were taken from gene sets already present in the MSig database of the Broad Institute.

Retroviral infection of $Lineage^{neg}cKit^{+}$ bone marrow cells or LSK cells. Bone marrow cells were enriched for cKit-positive cells using either the EasySep kit (StemCell Technology) or the Dynabead kit (DYNAL, Invitrogen). LSK cells were flow sorted using lineage markers Mac-1, Gr-1, NK1.1, TER-119, CD3, CD19, Sca1 and cKit. Cells were subsequently cultured in OPTI-MEM supplemented with 10% fetal bovine serum, 100 μg ml^{-1} penicillin, 100 μg ml^{-1} streptomycin, 50 ng ml^{-1} SCF and Flt3l, and 10 ng ml^{-1} IL-6 and IL-7. For retroviral production, Plat-E cells were transfected with appropriate retroviral expression constructs by the calcium phosphate method. Virus supernatant was collected 48 h after transfection and used directly for spin infection of cKit positive-enriched bone marrow cells or sorted LSK cells at 660*g* for 90 min. Forty-eight hours after infection, lineage-negative GFP-positive cells were sorted for RT–PCR analysis, methylcellulose plating assays or OP9 co-culture assay.

***In vitro* differentiation assays.** Total bone marrow (15,000), sorted LSK (500) and GMP (500) cells were plated in triplicates into cytokine-supplemented methylcellulose medium (MethoCult 3434, Stem Cell Technologies). Colony type was scored after 10 days of culture. Replating was performed after 8 days of culture. For experiments involving Hes1 overexpression, 10,000 GFP^{+} infected cells were plated in duplicate on 35 mm cytokine-supplemented methylcellulose medium (MethoCult 3434, Stem Cell Technologies). Cells were recovered 8 days later, stained and analysed by FACS as described.

Human progenitor/OP9 co-cultures. Bone marrow samples were obtained and used according to the guidelines of the Medical Ethical Commission of Ghent University Hospital (Belgium). Bone marrow mononuclear cells were isolated through Lymphoprep density-gradient centrifugation and $CD45^{+}$ glycophorin-A positive ($Gly\text{-}A^{+}$) cells were enriched by micro-magnetic beads (Miltenyi Biotec). Subsequently, $CD45^{+}Gly\text{-}A^{+}$ cells were labelled with CD34-FITC, CD38-PE, CD19-APC and CD14-APC to sort $CD34^{+}CD38^{-}Lin^{-}$ cells on a FACSAria to a purity greater than 98%. OP9-control and OP9 cells expressing human ligands Dll1, Dll4, Jag1 and Jag2 were generated by retroviral transduction of OP9 cells (provided by J. C. Zúñiga-Pflücker), followed by sorting for $eGFP^{+}$ cells, as described previously[31]. Purified bone-marrow progenitors (2.0×10^{3} – 2.6×10^{3}) were seeded into a 24-well plate with confluent OP9 cells in the presence of 20 ng ml^{-1} SCF, 20 ng ml^{-1} Flt-3L, 20 ng ml^{-1} TPO, 10 ng ml^{-1} GM-CSF and 10 ng ml^{-1} G-CSF. Co-cultures were performed and prepared for analysis as described previously[32]. Flow cytometric analysis was performed on an LSRII (BDIS). Human cells were gated using a CD45 monoclonal antibody and dead cells were excluded using propidium iodide.

OP9-DL1/DL4 *in vitro* co-culture. OP9 cells were maintained in MEM with 20% fetal bovine serum. Ten thousand purified infected (GFP^{+}) LSK or $cKit^{+}$ bone marrow progenitors were seeded into a six-well plate with confluent OP9 cells in the presence of 10 ng ml^{-1} SCF, 10 ng ml^{-1} IL-3, 10 ng ml^{-1} IL-6, 5 ng ml^{-1} Flt3-L and 5 ng ml^{-1} IL-7. Flow cytometric analysis was performed on an LSRII (BDIS). Haematopoietic cells were gated using CD45 cell-surface expression and GFP expression.

Chromatin immunoprecipitation assays. Chromatin immunoprecipitation assays were performed with 80 μg of genomic DNA from 32D-MIG- or 32D-HES1-infected cells following standard procedures. Briefly, chromatin was cross-linked with 1% formaldehyde, and sheared by sonication. Immunoprecipitation was performed with immunoglobulin-G or anti-HES1, followed by incubation with protein A magnetic beads/salmon sperm DNA (Invitrogen Dynal). DNA isolated from antibody bound fraction was eluted after washing, extracted with phenol/chloroform and precipitated with ethanol. Real-time PCR quantification of immunoprecipitated DNA was performed with the SYBR Green PCR Master Mix (Roche) and primers designed to amplify regions covering each putative HES1 binding site in the *Pu.1* and *Cebpa* promoters: Pu.1-1 forward ACGTTCAAGGGTTGGAGAAA, Pu.1-1 reverse GCCAATTAGGGCCAACAGTA; Pu.1-2 forward GACCAAAGTCCT CCACCTGA, Pu.1-2 reverse CTGGGAGGGAGAAAGGCTA; Cebpa-1 forward CCAAAGCAGTCTCCAACCTC, Cebpa-1 reverse CCCACTTCCAGCCAACAC TA; Cebpa-2 forward CGCCTAACCACGGACCAC, Cebpa-2 reverse AGTAG GATGGTGCCTGCTG.

Histological analyses. Mice were killed and autopsied, then dissected tissue samples or tumours were fixed for 24 h in 10% buffered formalin, dehydrated and embedded in paraffin. Paraffin blocks were sectioned at 5 μm and stained with haematoxylin and eosin.

Luciferase reporter assays. pGL3 promoter reporter plasmid (Promega) was used to clone Pu.1, Cebpa or Hes1 promoter sequences. pGL3 promoter empty vector or the vector containing Pu.1, Cebpa or Hes1 promoter sequences, HA-HES1 expression plasmid or pcDNA3.1 control plasmid and *Renilla* expression vector

were co-transfected into HEK293T cells using regular calcium phosphate transfection protocol. Luciferase activities were examined 24 h after transfection using the Dual Luciferase reporter assay system (Promega) following the manufacturer's instructions, and normalized to *Renilla* activity.

Statistical analysis. The means of each data set were analysed using Student's *t*-test, with a two-tailed distribution and assuming equal sample variance.

23. Yang, X. *et al.* Notch activation induces apoptosis in neural progenitor cells through a p53-dependent pathway. *Dev. Biol.* **269,** 81–94 (2004).
24. Saito, T. *et al.* Notch2 is preferentially expressed in mature B cells and indispensable for marginal zone B lineage development. *Immunity* **18,** 675–685 (2003).
25. Mitchell, K. J. *et al.* Functional analysis of secreted and transmembrane proteins critical to mouse development. *Nature Genet.* **28,** 241–249 (2001).
26. Leighton, P. A. *et al.* Defining brain wiring patterns and mechanisms through gene trapping in mice. *Nature* **410,** 174–179 (2001).
27. Rodriguez, C. I. *et al.* High-efficiency deleter mice show that FLPe is an alternative to Cre-loxP. *Nature Genet.* 25, 139–140 10.1038/75973 (2000).
28. Thompson, B. J. *et al.* Control of hematopoietic stem cell quiescence by the E3 ubiquitin ligase Fbw7. *J. Exp. Med.* **205,** 1395–1408 (2008).
29. Subramanian, A. *et al.* Gene set enrichment analysis: a knowledge-based approach for interpreting genome-wide expression profiles. *Proc. Natl Acad. Sci. USA* **102,** 15545–15550 (2005).
30. Mootha, V. K. *et al.* PGC-1α-responsive genes involved in oxidative phosphorylation are coordinately downregulated in human diabetes. *Nature Genet.* **34,** 267–273 (2003).
31. Van de Walle, I. *et al.* An early decrease in Notch activation is required for human TCR-αβ lineage differentiation at the expense of TCR-γδ T cells. *Blood* **113,** 2988–2998 (2009).
32. Taghon, T. *et al.* Notch signaling is required for proliferation but not for differentiation at a well-defined β-selection checkpoint during human T-cell development. *Blood* **113,** 3254–3263 (2009).